

## Operating Characteristics in DIII-D ELM-Suppressed RMP H-modes with ITER Similar Shapes

T.E. Evans 1), M.E. Fenstermacher 2), M. Jakubowski 3), R.A. Moyer 4), T.H. Osborne 1), M.J. Schaffer 1), O. Schmitz 5), J.G. Watkins 6), L. Zeng 7), L.R. Baylor 8), J.A. Boedo 4), K.H. Burrell 1), J.S. deGrassie 1), P. Gohil 1), I. Joseph 2), C.J. Lasnier 2), A.W. Leonard 1), S. Mordijck 4), C.C. Petty 1), R.I. Pinsky 1), T.L. Rhodes 7), J.C. Rost 9), P.B. Snyder 1), E. Unterberg 10), and W.P. West 1)

- 1) General Atomics, P.O. Box 85608, San Diego, California 92186-5608, USA
- 2) Lawrence Livermore National Laboratory, Livermore, California 94550, USA
- 3) Max-Planck-Institut für Plasmaphysik, Greifswald, Germany
- 4) University of California-San Diego, La Jolla, California 92093, USA
- 5) Forschungszentrum Jülich, IEF4-Plasmaphysik, Association EURATOM-FZJ, 52425 Jülich, Germany
- 6) Sandia National Laboratories, Albuquerque, New Mexico 94551, USA
- 7) University of California, Los Angeles, California 90095, USA
- 8) Oak Ridge National Laboratory, Oak Ridge, Tennessee 37831, USA
- 9) Massachusetts Institute of Technology, Cambridge, Massachusetts 02139, USA
- 10) Oak Ridge Institute for Science Education, Oak Ridge, Tennessee 37831, USA

e-mail contact of main author: [evans@fusion.gat.com](mailto:evans@fusion.gat.com)

**Abstract.** Fast energy transients, incident on the DIII-D divertors due to Type-I edge localized modes (ELMs), are eliminated using small dc currents in a simple set of non-axisymmetric coils that produce edge resonant magnetic perturbations (RMP). In ITER similar shaped (ISS) plasmas, with electron pedestal collisionalities matched to those expected in ITER a sharp resonant window in the safety factor at the 95 percent normalized poloidal flux surface is observed for ELM suppression at  $q_{95}=3.57$  with a minimum width  $\delta q_{95}$  of  $\pm 0.05$ . The size of this resonant window has been increased by a factor of 4 in ISS plasmas by increasing the magnitude of the current in an  $n=3$  coil set along with the current in a separate  $n=1$  coil set. The resonant ELM-suppression window is highly reproducible for a given plasma shape, coil configuration and coil current but can vary with other operating conditions such as  $\beta_N$ . Isolated resonant windows have also been found at other  $q_{95}$  values when using different RMP coil configurations. For example, when the I-coil is operated in an  $n=3$  up-down asymmetric configuration rather than an up-down symmetric configuration a resonant window is found near  $q_{95}=7.4$ . A Fourier analysis of the applied vacuum magnetic field demonstrates a statistical correlation between the Chirikov island overlap parameter and ELM suppression. These results have been used as a guide for RMP coil design studies in various ITER operating scenarios.

### 1. Introduction

Type-I edge localized modes (ELMs) [1] are a significant concern in magnetically confined toroidal fusion plasmas because they can rapidly erode plasma facing material surfaces, reduce the coupling efficiency of radio frequency antennas, cause noise in feedback circuits used to control core-MHD modes and interfere with diagnostic measurements of critical operating parameters. ELMs have been suppressed in the DIII-D [2] tokamak over a wide range of pedestal collisionalities  $\nu_e^* = q_{95} R \varepsilon^{-3/2} \lambda_e^{-1}$  [3] and plasma shapes with resonant magnetic perturbations (RMPs) that have toroidal mode number  $n=3$  [4,5]. Here,  $R$  is the major radius,  $\varepsilon$  ( $\equiv a/R$ ) is the inverse aspect ratio,  $a$  is the minor radius and  $\lambda_e$  ( $=v_{Te}\tau_e$ , the product of electron thermal velocity  $v_{Te}$  and collision time  $\tau_e$ ) is the mean free path for electron collisions. In high average triangularity  $\bar{\delta} = (\delta_{\text{upper}} + \delta_{\text{lower}})/2 = 0.54$  plasmas with moderate collisionalities  $\nu_e^* \approx 1$ , Type-I ELMs are replaced by small intermittent events with a coherent amplitude modulation of  $\sim 130$  Hz [4,6]. In these discharges, an  $n=3$  up-down asymmetric RMP pulse with a peak vacuum field spectral amplitude approximately equal to

that of the edge DIII-D field-errors ( $\delta b_r^{(11,3)} = 0.4G$ ) is used to create a dense set of vacuum magnetic islands across the pedestal. These islands are produced by an RMP from the DIII-D I-coil [7] and have poloidal mode numbers ranging from  $m=9$  to  $m=14$  across the pedestal when the safety factor on the 95% normalized flux surface  $q_{95}$  is between 3.5 and 3.9. In these moderate collisionality plasmas, ELMs are suppressed by the applied RMP without any appreciable change in the pedestal pressure profile [4,8] once the  $q_{95}$  resonance condition is satisfied. This suggests that the RMP fields either couples directly to the eigenmode structure of the ELMs or modifies the ELM stability threshold in a way that is not easily observed experimentally.

In low collisionality plasmas with  $0.1 \leq v_e^* \leq 0.2$  and an average triangularity  $\bar{\delta} \leq 0.26$ , ELMs are completely eliminated over a  $q_{95}$  resonant window ranging from 3.55 to 3.85. Outside this  $q_{95}$  range ELMs are typically reduced in amplitude by as much as a factor of 4 and are increased in frequency by up to a factor of 13. We refer to this behavior as ELM mitigation as opposed to full ELM suppression obtained when the  $q_{95}$  resonance condition is satisfied. The minimum  $m,n=11,3$  RMP spectral amplitude required for ELM suppression in low collisionality, low triangularity, plasmas lies between  $\delta b_r^{(11,3)} B_T^{-1} = 1.7 \times 10^{-4}$  and  $\delta b_r^{(11,3)} B_T^{-1} = 2.6 \times 10^{-4}$  with  $n=3$ , up-down symmetric, I-coil currents of 2 and 3 kA respectively depending on operating conditions such as  $\beta_N$  [9]. Here,  $B_T = 1.9T$  is the toroidal magnetic field on axis. This calculated RMP field amplitude these low collisionality plasmas is  $\sim 8-9$  times larger than that required in the  $\bar{\delta} = 0.54$   $v_e^* \approx 1$  case discussed above and does not include effects of the plasmas response to the field [10,11]. In low  $v_e^*$  plasmas, ELMs are suppressed by a reduction in the pedestal pressure profile caused by the application of the RMP field. The pedestal pressure is reduced by a change in the global particle balance which reduces the density without appreciably affecting the edge  $T_e$  profile [4,9,12]. The ion temperature in these plasmas increases substantially during the RMP pulse with a typical central  $T_i$  of  $\sim 15-18$  keV. In the pedestal, the total pressure gradient is reduced by the reduction in density which moves the operating point into a stable region of peeling-ballooning mode parameter space [13].

A significant difference in the response of the plasma to the  $n=3$  RMP fields is observed in ISS (ITER Similar Shaped) discharges compared to low collisionality, low triangularity plasmas [14]. An example of the plasma response to the RMP field in this configuration is shown in Fig. 1.

In 2006 the DIII-D lower divertor baffle was extended to allow improved pumping in high triangularity plasmas. This made it possible to carry out RMP ELM control experiments in low ( $v_e^* \leq 0.2$ ) collisionality plasmas with

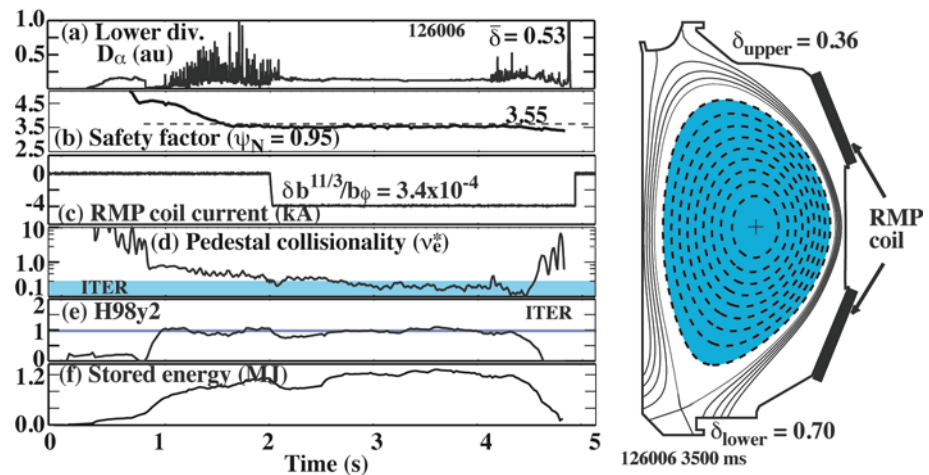


FIG. 1. Example of full ELM suppression in a low collisionality, high average triangularity DIII-D ISS plasma (discharge 126006). The plasma shape (right) at  $t = 3500$  ms is shown along with the location of the RMP coil (i.e., the DIII-D I-coil). On the left: (a) a typical lower divertor  $D_\alpha$  signal is shown along with (b) the evolution of  $q_{95}$ , (c) the RMP coil current, (d) the pedestal collisionality, (e) the H-factor and (f) the stored energy.

an average triangularity  $\bar{\delta} \leq 0.53$ . In these plasmas the minimum  $m, n = 11, 3$  RMP spectral amplitude required for ELM suppression increased to  $\delta b_r^{(11,3)} B_T^{-1} = 3.4 \times 10^{-4}$  as shown in Fig. 1(c). This increase in the RMP field compared to the low triangularity configurations is due to a narrowing of the safety factor profile and an increase in the magnetic shear across the pedestal when operating in the ISS configuration. In addition, the distance from the lower I-coil to the resonant surfaces across the pedestal increased in ISS plasmas.

In this paper, we focus on the operating characteristics of ELM suppressed H-modes with RMP fields, referred to as RMP H-modes, and describe results that provide insight into how this approach may scale to future devices such as ITER. Section 2 covers the properties of the ELM suppression resonant window. Section 3 describes the relationship between the width of the edge island overlap region and ELM suppression while Section 4 describes results using various RMP coil configurations, impurity effects and observations during core pellet fueling experiments. Section 5 provides a summary of the results and conclusions.

## 2. Resonant ELM Suppression Window

A characteristic feature of complete ELM suppression, as opposed to simply reducing the amplitude of the ELMs, is a resonant  $q_{95}$  window. We refer to this as a resonant window because it has a sharp upper and lower bound. The characteristics of this resonant window are shown in Fig. 2 for an ISS plasma with an  $n=3$  I-coil pulse. In addition to the  $n=3$  RMP field from the I-coil, most DIII-D experiments are run with  $n=1$  field-error corrections from the C-coil as well as  $n=1, 2$  and  $3$  field-errors from various sources intrinsic to the machine. In the pedestal region, field-error related RMP sources are typically an order of magnitude smaller than the  $n=3$  I-coil fields. The existence of a sharp  $q_{95}$  resonant window is a common feature of the ELM suppression process in each plasma shape and collisionality regime used for these experiments although the width and mean value of the window varies somewhat

with the plasma shape and other operating parameters [14]. It has also been shown that the details of the safety factor profile, such as the location of the  $q=3$  surface and edge shear, have a significant effect on the width and mean value of the window [14].

As shown in Fig. 2, a downward  $q_{95}$  ramp results in full ELM suppression when  $q_{95} = 3.57 \pm 0.05$ . Given the geometry of the internal RMP coil in DIII-D (the I-coil), this resonant window is seen with a coil configuration referred to as even parity (up-down symmetric with respect to the equatorial plane of DIII-D) and a current in the single-turn coil loops of 4.0 kA. With the coil configured for odd parity operations (upper and lower pairs giving oppositely directed perturbations) ELM suppression is also obtained with  $q_{95} \sim 7.2$ . Increasing the  $n=3$  RMP strength (I-coil current) increases the width of the resonance window for suppression. In addition, increasing the magnitude of  $n=1$  field from the external field-error correction coil (the C-coil), in combination with sufficiently strong  $n=3$  RMP fields, also increases the width of the resonance window in  $q_{95}$  for ELM suppression. When these two RMP coils are combined in this way the C-coil is used to increase the width of the intrinsic  $m, n=3, 1$  and  $4, 1$  magnetic islands produced by field-errors and the I-coil is used to increase the widths of the

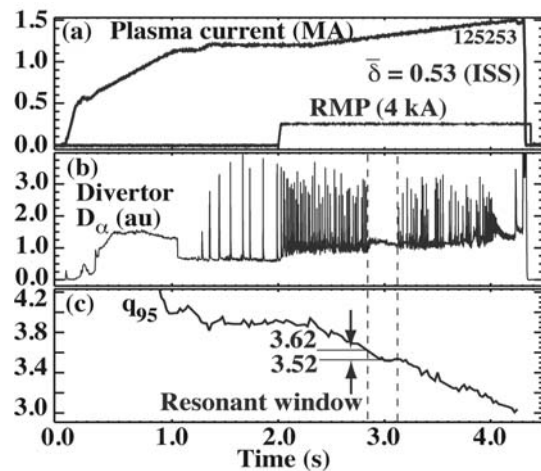


FIG. 2. An example of sharp  $q_{95}$  ELM suppression window in an ISS plasma with (a) an upward  $I_p$  ramp and 4 kA  $n=3$  RMP I-coil pulse producing (b) a quiescent interval in the lower divertor  $D_\alpha$  as (c)  $q_{95}$  passes through the region bounded by 3.62 and 3.52 during the downward ramp.

$m,n=8,3$  through  $11,3$  magnetic islands to fill-in gaps across the pedestal where the islands do not quite overlap. An example of the increase seen in the width of the  $q_{95}$  resonant window from ELM suppression is shown in Fig. 3. For the discharge conditions used in these experiments, the resonant ELM suppression window increases from  $q_{95} = 3.525 \pm 0.055$  with 3 kA in the I-coil ( $n=3$ , even parity) and an average current of 1.3 kA (5.2 kAt) in the  $n=1$  C-coil to  $q_{95} = 3.475 \pm 0.225$  with 4 kA in the I-coil and an average current of 2.6 kA in the  $n=1$  C-coil [15]. This factor of 4 increase in the width of the resonant window requires less than a factor of 2 increase in the RMP field amplitude suggesting a somewhat stronger than quadratic scaling with the RMP coil current when combining  $n=3$  perturbations with  $n=1$  perturbations.

Although ELMs are not suppressed when operating above the  $q_{95}$  resonant window, the ELM frequency and amplitude are significantly modified. We refer to this behavior as ELM mitigation, since the amplitude of the ELMs is reduced. An example of the ELM response to an  $n=3$  I-coil RMP field during a  $q_{95}$  scan in an ISS plasma is shown in Fig. 4. Here,  $q_{95}$  drops from 4.2 to 3.7 [Fig. 4(a)], where a 2,1 locked mode developed before ELM suppression is obtained at the upper edge of the resonant window. The toroidal CVI rotation at the top of the pedestal [Fig. 4(a)] remains relatively constant at  $\sim 45$  km/s as  $q_{95}$  drops except when a locked MHD mode develops at  $\sim 2.95$  s. We typically find that locked modes grow rapidly in ISS plasmas when the pedestal rotation drops below 40–45 km/s [14], which may be related to the penetration of intrinsic  $n=1$  field-errors into the core plasma as the rotation drops. As seen in Fig. 4(b), there is a monotonic decrease in the ELM amplitude with  $q_{95}$  during the I-coil pulse. Initially, the I-coil produces an ELM frequency of  $\sim 200$  Hz (compared to 25 Hz before the I-coil) with 38% of the  $D_\alpha$  magnitude compared to the ELMs before the I-coil pulse. By the end of the  $q_{95}$  ramp, the maximum  $D_\alpha$  magnitude due to the ELMs has dropped to  $\sim 27\%$  of the pre-RMP ELM magnitude and the frequency has increased to  $\sim 330$  Hz.

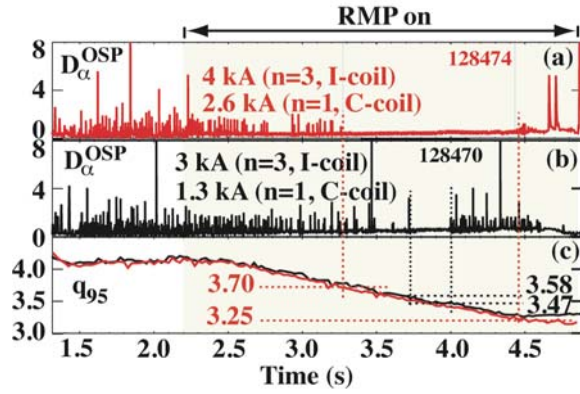


FIG. 3. Example of an increased  $q_{95}$  resonant window in two ISS plasma where the duration of the ELM suppressed phase in the lower divertor  $D_\alpha$  signal during a (a) 4 kA  $n=3$  I-coil combined with an average 2.6 kA  $n=1$  C-coil (discharge 128474) is significantly increased compared to (b) a 3 kA  $n=3$  I-coil combined with an average 1.3 kA  $n=1$  C-coil (discharge 128470) resulting in (c) a  $q_{95}$  resonant window ranging from 3.70 to 3.25 in discharge 128474 compared to 3.58 to 3.47 in discharge 128470.

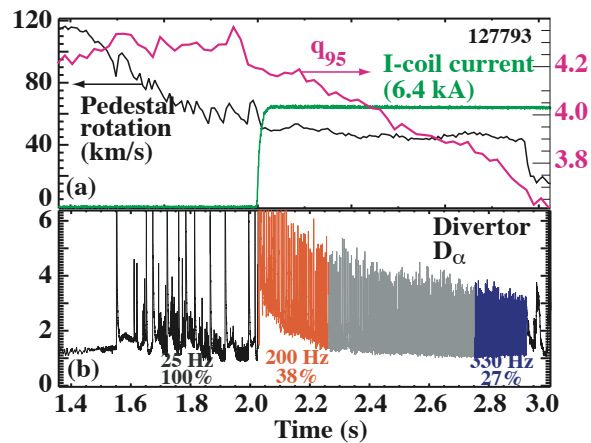


FIG. 4. Example of ELM mitigation in an ISS plasma where (a)  $q_{95}$  is ramped from 4.2 to 3.6 and the carbon VI toroidal rotation remains relatively constant (until a core MHD mode is destabilized a 2.9 s) during an  $n=3$  RMP pulse. Here, the (b) lower divertor  $D_\alpha$  signal that ELMs have a monotonically decreasing amplitude and increasing frequency during the RMP pulse compared to the Type-I ELM before the RMP pulse.

### 3. ELM Suppression vs the Vacuum Island Overlap Parameter

The existence of a sharp  $q_{95}$  resonant window suggests that the position of the last good Kolmogorov-Arnold-Moser (KAM) surface [16], between the outer stochastic layer and the inner isolated magnetic island region, may be key parameter that is needed to understand the physics involved in RMP H-modes [14]. In addition, when operating inside the resonant window, experimental observations show that changes in the total pressure gradient primarily affect the region inside the top of the pedestal (i.e.,  $0.80 \leq \psi_N \leq 0.95$ ) [14]. Detailed analysis of these effects has shown that under some plasma conditions the relative position of the last good KAM surface or its associated Chirikov parameter, as described below, is well correlated with the ELM suppression obtained in these ISS RMP H-modes [15].

The maximum ELM size observed during experiments with  $n=3$  RMP fields from both the upper and lower rows of the internal I-coil, at fixed  $q_{95}$ , is correlated with the width of the vacuum magnetic island overlap region [14,15]. To quantify the width of the overlap region we use the so-called Chirikov parameter which is defined as the sum of the half widths of neighboring islands divided by their separation  $\sigma_{\text{Chir}} = (W_{m,n} + W_{m+1,n})/2d_{(m,m+1),n}$ . Although the last good KAM surface is typically located at a normalized poloidal flux surface ( $\psi_N$ ) where  $\sigma_{\text{Chir}} < 1$ , we quantify the width of the vacuum stochastic flux loss layer in  $\psi_N$  as the point where a significant fraction of the boundary layer field lines (i.e., more than 10%) are lost from the pedestal and terminate on a divertor target plate. Thus, a criteria that can be used to order the ELM size versus the RMP field effectiveness is the width of the region in  $\psi_N$  over which  $\sigma_{\text{Chir}} \geq 1$  or  $(\Delta\psi_N)_{\sigma_{\text{Chir}}=1} = 1 - \psi_N(\sigma_{\text{Chir}} \geq 1)$ . As shown in Fig. 5, this criteria is an effective way to parameterize the peak  $D_\alpha$  signal seen at the inner divertor during ELMs, in ISS plasmas, with and without  $n=3$  RMP fields. Here, the peak signal is normalized to the largest Type-I ELM value without the  $n=3$  I-coil field. Note that even with zero I-coil current  $(\Delta\psi_N)_{\sigma_{\text{Chir}}} \neq 0$  due to the presence of intrinsic field-errors and the  $n=1$  C-coil field. At low

$n=3$  I-coil current ELMs are mitigated when  $(\Delta\psi_N)_{\sigma_{\text{Chir}}}$  ranges between  $\sim 0.1$  and  $\sim 0.16$ . Above  $(\Delta\psi_N)_{\sigma_{\text{Chir}}} \approx 0.16$  the normalized peak  $D_\alpha$  due to ELMs is essentially zero except for a few low level outliers. Of course, this is a vacuum field ordering parameter and the plasma response to the RMP may alter the relationship between the normalized peak  $D_\alpha$  and  $(\Delta\psi_N)_{\sigma_{\text{Chir}}}$ . Understanding the plasma response to the RMP is and area of active research in the international fusion community. Note that this correlation between the  $(\Delta\psi_N)_{\sigma_{\text{Chir}}}$  and the normalized peak  $D_\alpha$  does not always apply. For example, during  $q_{95}$  ramps when the edge bootstrap current is affected by changes in  $I_p$  the correlation is not as well defined. Nevertheless, the  $(\Delta\psi_N)_{\sigma_{\text{Chir}}}$  criteria provides us a reasonably good engineering parameter for scaling the DIII-D I-coil RMP fields to machines with similar coil designs such as ITER.

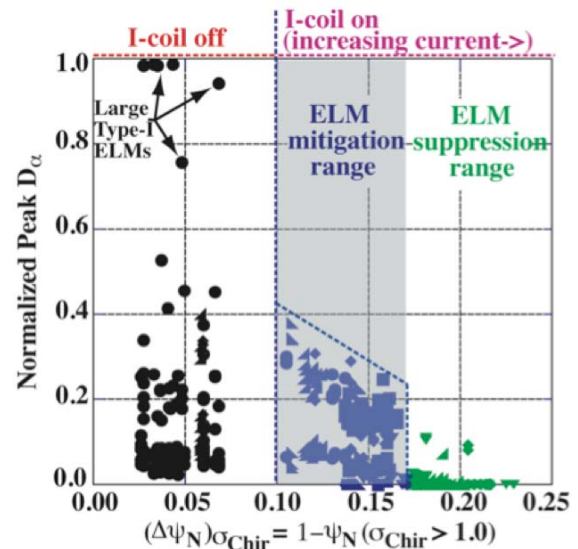


FIG. 5. The normalized peak in a divertor  $D_\alpha$  signal is well correlated with the width of the stochastic boundary layer when parameterized by the width of the region between the separatrix  $\psi_N = 1$  and the point in  $\psi_N$  where the Chirikov parameter crosses unity.

In addition to the width of the island overlap region, an analysis of the perturbed vacuum island structure on flux surfaces where  $\sigma_{\text{Chir}} < 1$  shows that a larger fraction of the field lines lost to the divertor target plates originate from a region near isolated magnetic islands when ELMs are suppressed as opposed to when they are simply mitigated with the applied  $n=3$  I-coil RMP fields [12,15]. This suggests that *ExB* convective cells could be associated with the remnant islands and may play a role in the particle transport during the RMP [12,17–19].

#### 4. Variations in the I-coil Configuration, Impurities & Pellet Fueling in RMP H-modes

ELM suppression is also obtained with  $n=3$  RMPs produced by only one row of the internal I-coil (i.e., either the upper or the lower row). To obtain Elm suppression with either the upper or lower row of the I-coil, the current in the single-row coil configuration must be increased to the point that RMP fields match the perturbation strength near the top of the pedestal produced with both rows of the I-coil as shown in Fig. 6 [20]. Attempts to obtain ELM suppression using  $n=3$  RMP fields from a single-row of large aperture, external coils located on the equatorial plane of DIII-D (i.e., the C-coil) with the same pedestal perturbation strength as was used with a single-row of the I-coil resulted in the onset of locked modes without obtaining ELM suppression. The maximum ELM size obtained during the application of an RMP from a single internal coil row, at fixed  $q_{95} = 3.6$ , is also correlated with the edge island overlap width, although the minimum width for achieving ELM suppression is smaller,  $(\Delta\psi_N)_{\sigma_{\text{Chir}}} \sim 0.12$ , than in the cases with both I-coil rows. This suggests that factors, other than achieving a minimum overlap width from vacuum island calculations, play a role in achieving the modification to the pedestal profiles necessary for ELM suppression [20,21].

During  $n=3$  RMP ELM suppressed H-modes in high triangularity ISS discharges, high recycling conditions in the divertor produce a low divertor impurity source and a relatively low core plasma  $Z_{\text{eff}}$  is maintained (i.e., levels comparable to the ELMing phase without the RMP) [14]. This is in contrast to the low recycling sheath limited divertor conditions observed in low average triangularity ( $\bar{\delta} \leq 0.26$ ), low collisionality, experiments where localized impurity sources resulted in significantly elevated core impurity levels during RMP H-modes [22]. Results in ISS plasmas have established that RMP H-modes with low core  $Z_{\text{eff}}$  can be achieved with ITER-like low pedestal collisionality. This result is believed to be due to a combination of factors including: 1) the high- $\bar{\delta}$  ISS geometry favors detachment of the inner strike-point and trapping of neutrals in the divertor is better (shorter ionization mfp) than in the low- $\bar{\delta}$  shape where both strike-points are on a flat divertor target, 2) the gaps between divertor target tiles were substantially reduced when the new high- $\bar{\delta}$  pumping baffle was installed in DIII-D between the two experiments, and 3) that ELMs are controlled in the high- $\bar{\delta}$  ISS RMP H-modes at somewhat higher density than for the low- $\bar{\delta}$  experiments. All of the beneficial factors observed in ISS RMP H-modes are well matched

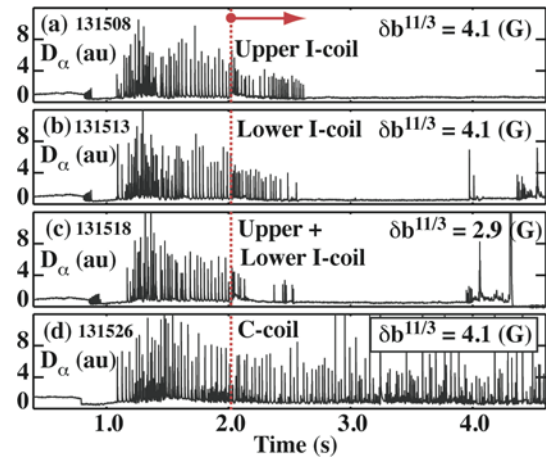


FIG. 6. Lower divertor  $D_\alpha$  signals showing ELM suppression with an  $n=3$  RMP from the: (a) upper-row of the I-coil (an internal, small aperture, coil), (b) the lower-row of the I-coil and (c) both the upper and lower rows of the I-coil. Part (d) shows the same  $D_\alpha$  signal for a discharge with an  $n=3$  C-coil (an external, large aperture, coil centered on the equatorial plane) RMP that has an  $m,n=11,3$  perturbation field at the top of the pedestal which is equivalent to that use in the single-row I-coil cases (a) and (b).

with the expected operating parameters in ITER, providing an optimistic outlook for core impurity control during ITER RMP H-modes.

A key issue for RMP H-mode operations is whether core pellet fueling, a requirement in ITER, will destabilize ELMs. It has been shown that several small  $D_\alpha$  transients follow the injection of a HFS deuterium fueling pellet in DIII-D [14]. It was also shown that the core density increases following a fueling pellet without the return of continuous ELMs. Experiments in ISS plasmas have demonstrated that the core density can be increased in DIII-D RMP H-modes by approximately a factor of 2 by injecting core fueling pellets with a repetition rate of 5 Hz, without initiating periods of sustained ELMs (although several small  $D_\alpha$  transients were observed following each pellet). Several attempts to increase the pellet repetition rate to 10 Hz caused a sustained period of ELMs following each pellet. As shown in Fig. 7, it is possible to achieve robust RMP H-modes that are immune to these  $D_\alpha$  transients. It is interesting to note that the transients may result from increasing the RMP fields which appears to produce a prompt loss of the ablated pellet mass. By reducing the current in the RMP coil these transients can be essentially eliminated as seen in Fig. 7(b).

## 5. Summary and Conclusions

Type-I ELMs are either completely suppressed or mitigated by  $n=3$  RMP fields produced by the internal DIII-D I-coil in a variety of plasma shapes and collisionalities. A common feature of complete ELM suppression is the existence of a sharp  $q_{95}$  resonant window that can range from  $q_{95} = 3.57 \pm 0.05$  to  $q_{95} = 3.475 \pm 0.225$  during plasma current ramping experiments depending on the RMP coil configuration and plasma parameters such as  $\beta_N$ , shape and wall conditions. The width and mean value of the resonant window is increased by increasing the current in the I-coil or by adding  $n=1$  RMP fields from the external  $n=1$  field-error correction coil (i.e., DIII-D C-coil). ELMs are also suppressed with a single-row of the internal I-coil (a small-aperture coil located off the equatorial plane) when the current is increased to the point that the RMP field at the top of the pedestal is equivalent to that produced with the two-row I-coil configuration. Attempts to suppress ELMs with  $n=3$  fields from the external C-coil (a larger-aperture coil located on the equatorial plane) resulted in locked modes before ELM suppression could be achieved although an equivalent RMP field was obtained at the top of the pedestal just as in the single-row I-coil configuration.

The existence of a resonant  $q_{95}$  window for ELM suppression in addition to changes seen in the pressure profile from the top of the pedestal inward led to the development of a vacuum island overlap criteria which provides a good engineering parameter for scaling DIII-D I-coil results to similar coil geometries in other tokamaks such as ITER. A good correlation

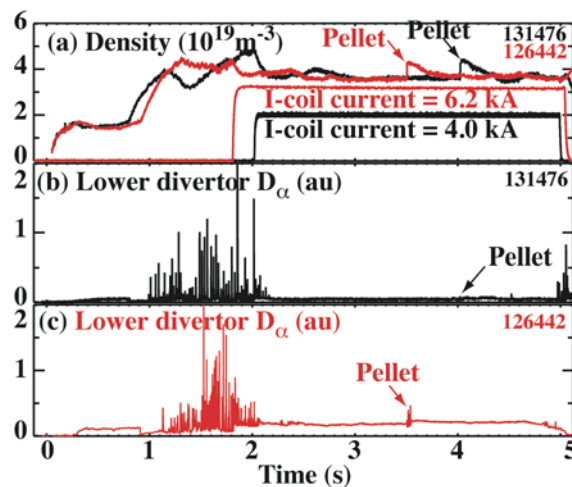


FIG. 7. Although the core density is reduced during the I-coil pulse as shown in (a) for discharge 126442 with an I-coil current of 6.2 kA and for discharge 131476 with an I-coil current of 4.0 kA, it is recovered transiently when a core fueling pellet is injected from the high field side of the discharge. In discharge 131476 the (b) lower divertor  $D_\alpha$  signal does not show the small transients following the pellet injection seen in the (c) lower divertor  $D_\alpha$  signal following the pellet in discharge 126442. Note that in both discharges a sustained ELMing period is not destabilized by the pellet even though the core density remains near the pre-RMP level for several Type-I ELM periods.

between the normalized peak  $D_\alpha$  in the divertor due to an ELM and the width of the vacuum stochastic layer (where the Chirikov parameter is equal to or greater than unity) is found in ISS plasmas with stationary  $q_{95}$  values inside the resonant window for ELM suppression. Significant progress has been made on developing RMP ELM suppressed operating conditions in ITER relevant plasmas and shapes, including an ability to increase the density by a factor of 2 using 5 Hz core pellet fueling without initiating periods of sustained ELMs. RMP H-modes have been obtained in which core-fueling pellets do not trigger small  $D_\alpha$  transients following the injection of a single pellet and it has been shown that core impurity levels are not significantly higher in ISS RMP H-modes than those in ELMing H-modes. While a detailed physics understanding of all the effects seen in RMP H-modes is still developing, the results presented here provide an increased level of confidence for achieving robust RMP H-modes in ITER.

This work was supported by the US Department of Energy under DE-FC02-04ER54698, DE-AC52-07NA27344, DE-FG02-07ER54917, DE-AC04-94AL85000, DE-FG03-01ER54615, DE-AC05-00OR22725, DE-AC05-76OR00033 and DE-FG02-05ER54809.

## References

- [1] FENSTERMACHER, M.E., *et al.*, Plasma Phys. Control. Fusion **45**, 1597 (2003).
- [2] LUXON, J.L., Nucl. Fusion **42**, 614 (2002).
- [3] LOARTE, A., *et al.*, Plasma Phys. Control. Fusion **45**, 1549 (2003).
- [4] EVANS, T.E., *et al.*, Phys. Rev. Lett. **92**, 235003-1 (2004).
- [5] EVANS, T.E., *et al.* Nature Physics **2**, 419 (2006).
- [6] MOYER, R.A., *et al.*, Phys. Plasmas **12**, 056119 (2005).
- [7] JACKSON, G.L., *et al.*, Proc. of 30th EPS Conf. on Plasma Physics, St. Petersburg (2003) P-4.47.
- [8] EVANS, T.E., *et al.*, Nucl. Fusion **45**, 595 (2005).
- [9] BURRELL, K.H., *et al.*, Plasma Phys. Control. Fusion **47**, B37 (2005).
- [10] FITZPATRICK, R., Phys. Plasmas **5**, 3325 (1998).
- [11] BOOZER, A., Phys. Plasmas **12**, 0925404 (2005).
- [12] EVANS T.E., *et al.*, Phys. Plasmas **13**, 056121 (2006).
- [13] OSBORNE, T.H., *et al.*, Proc. of 32nd EPS Conf. on Plasma Physics, Tarragona, Spain (2005) P-4.012.
- [14] EVANS, T.E., *et al.*, Nucl. Fusion **48**, 024002 (2008).
- [15] FENSTERMACHER, M.E., *et al.*, Phys. Plasmas **15**, 056122 (2008).
- [16] LICHTENBERG, A.J., *et al.*, Applied Mathematical Science **38**, Springer-Verlag (1983).
- [17] TAKAMURA, S., *et al.*, Phys. Fluids **30**, 144 (1987).
- [18] EVANS, T.E., *et al.*, Proc. of 14th EPS Conf. on Plasma Physics, Madrid, Spain (1987) Vol. 11D, p.770.
- [19] McCOOL, S.C., *et al.*, Nucl. Fusion **30**, 167 (1990).
- [20] FENSTERMACHER, M.E., *et al.*, Nucl. Fusion submitted (2008).
- [21] FENSTERMACHER, M.E., *et al.*, J. Nucl. Mater. submitted (2008).
- [22] FENSTERMACHER, M.E., *et al.*, J. Nucl. Mater. **363-365**, 476 (2007).